Microelectronic Engineering 85 (2008) 2299–2303

Contents lists available at ScienceDirect

Microelectronic Engineering

journal homepage: www.elsevier.com/locate/mee

Effect of 6 MeV electron irradiation on electrical characteristics of the Au/*n*-Si/Al Schottky diode

E. Uğurel [a], Ş. Aydoğan [a,*], K. Şerifoğlu [b], A. Türüt [a]

[a] Department of Physics, Faculty of Sciences and Arts, University of Atatürk, 25240 Erzurum, Turkey
[b] Department of Radiation Oncology, Faculty of Medicine, Atatürk University, 25240 Erzurum, Turkey

ARTICLE INFO

Article history:
Received 1 May 2008
Received in revised form 19 July 2008
Accepted 21 August 2008
Available online 31 August 2008

Keywords:
Electron irradiation
Schottky contact
Schottky barrier
Series resistance

ABSTRACT

Electron irradiation of the Au/*n*-Si/Al Schottky diode was performed by using 6 MeV electrons and 3×10^{12} e^-/cm^2 fluency. The current–voltage (*I–V*), capacitance–voltage (*C–V*) and capacitance–frequency (*C–f*) characteristics of the unirradiated and irradiated Schottky diode were analyzed. It was seen that the values of the barrier height, the series resistance, and the ideality factor increased after electron irradiation. However, there was a decrease in the leakage current with electron irradiation. The increase in the barrier height and in the series resistance values was attributed to the dopant deactivation in the near-interface region. The interface states, N_{ss}, have been decreased significantly after electron irradiation. This was attributed to the decrease in recombination centre and the existence of an interfacial layer. A decrease in the capacitance was observed after electron irradiation. This was attributed to decrease in the net ionized dopant concentration with electron irradiation.

© 2008 Elsevier B.V. All rights reserved.

1. Introduction

Recently, the studies of the radiation damage of the semiconductor-based devices have increasingly demanded the attention of researchers. Although the impact of the radiation on the performance of the devices have clearly been known as various deformations, there is yet no convenient explanation to all types of crystals or devices. There are two types of basic radiation-damage mechanisms for devices: ionisation damage and displacement lattice damage. Ionisation of the material creates free charge, which can move in the material. This damage is generally harmless for the device operation. But displacement lattice damage in semiconductor-based devices can have a significant impact on their electrical properties, through the creation of stable radiation defects, which have one and/or more levels in the bandgap. Free carrier mobility and density, resistivity, and generation and recombination lifetimes will be affected by displacement lattice damage. After irradiation, an increase in the resistivity is mostly observed, which results from the various effects. For example, the removal and/or reduction of the free carriers occurs due to either direct removal of dopants from active (substitutional) lattice sites by interaction with the created vacancies and interstitials giving rise to a stable point defect complexes or dopants in a "neutral" (i.e. interstitial) lattice site. Well-known examples for silicon are the creation of group V donor–vacancy pairs or the creation of interstitial [1–4]. In some cases, the type inversion may occur (from *n*- to *p*-type or reverse, by removing the charge carriers) or the presence of radiation-induced deep levels changes the charge balance in the device and the position of the Fermi level in the semiconductor, which impacts on the net free carrier density. In many cases, the charge of the shallow dopants is compensated by the radiation levels, resulting in a lowering of the free carrier density and an increase in resistivity [5]. The radiation-induced damage is also directly related to the amount of energy and radiation fluency absorbed by the device material or the total dose of radiation received by the device. Therefore, it is important to determine how the Schottky contact parameters give a response to the high-energy electron irradiation, since all semiconductor-based devices communicate one another over the metal/semiconductor (MS) contacts in an electronic circuit [6]. The effect of 6 MeV electron irradiation on the *I–V*, *C–V-F* characteristics of Au/*n*-Si/Al Schottky contact has been studied and reported in this article.

2. Experimental

We have used a *n*-type Si semiconductor wafer with (100) orientation, 400 μm thickness and 1–10 Ω-cm resistivity. Before making contacts, the wafer was chemically cleaned using the RCA cleaning procedure (i.e. 10 min boil in $NH_3 + H_2O_2 + 6H_2O$ followed by a 10 min $HCl + H_2O_2 + 6H_2O$ at 60 °C). Extensive alloys such as Au–Sb are used for *n*-Si ohmic contact. We have used Al for ohmic contact by evaporating on *n*-Si wafer. Then, it was annealed at 525 °C for 15 min in N_2 atmosphere. The native oxide on the front surface of substrate was removed in $HF + 10H_2O$ solution. Finally, it

* Corresponding author.
E-mail addresses: saydogan@atauni.edu.tr, saydogan43@yahoo.com (Ş. Aydoğan).

0167-9317/$ - see front matter © 2008 Elsevier B.V. All rights reserved.
doi:10.1016/j.mee.2008.08.002

was rinsed in deionized water for 30 s and was dried. Then, Au was evaporated on the n-Si at 10^{-5} torr (diode area = 7.85×10^{-3} cm^2). The I–V and C–V/f measurements of Au/n-Si/Al Schottky diode were performed with KEITLEY 487 Picoammeter/Voltage Source and HP 4192A (50 Hz to 13 MHz) LF IMPEDENCE ANALYZER at room temperature, and in dark.

3. Results and discussion

Fig. 1 shows the forward and reverse bias I–V characteristics of the diode before and after irradiation. The effect of irradiation is clearly shown. Both I–V characteristics show that they are dominated by the series resistance at higher voltage values. It is seen that after electron irradiation in the diode, leakage current has been decreased. The other effect of irradiation is a reduction in a forward bias current.

The current through a homogeneous SBD at a forward bias V is described within the thermionic emission–diffusion (TED) theory by [7]

$$I = AA^*T^2\exp\left(-\frac{q\Phi_b}{kT}\right)\left[\exp\left(\frac{qV}{nkT}\right)-1\right], \tag{1}$$

where

$$I_0 = AA^*T^2\exp\left(\frac{-q\Phi_b}{kT}\right) \tag{2}$$

is the saturation current, Φ_b is the effective barrier height at zero bias, A^* is the Richardson constant and equals 112 A/cm^2 K^2 for n-type Si, where q is the electron charge, V is the applied voltage, A is the diode area, k is the Boltzmann constant, T is the temperature in Kelvin, n is the ideality factor, and it is determined from the slope of the linear region of the forward bias ln$I$–V characteristic through the relation

$$n = \frac{q}{kT}\frac{dV}{d(\ln I)}, \tag{3}$$

where n equals unity for an ideal diode. However, n has usually a value greater than unity. High values of n can be attributed to the presence of the interfacial thin native oxide layer, to a wide distribution of low-SBH patches (or barrier inhomogeneities) and to the bias voltage dependence of the SBH [7].

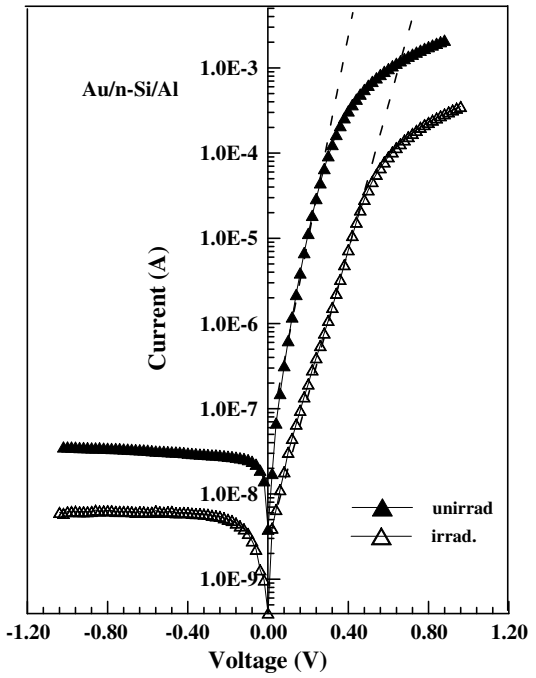

Fig. 1. The C–V characteristics of the Au/n-Si/Al Schottky diode before and after irradiation.

Φ_b is the zero-bias barrier height (BH), which can be obtained from the following equation:

$$\Phi_b = kT/q\ln(AA^*T^2/I_0). \tag{4}$$

The values of the barrier heights for before and after irradiation are calculated as 0.73 and 0.80 eV, respectively. Furthermore, the values of the ideality factors for before and after irradiation are calculated as 1.44 and 1.96 eV, respectively. It is seen that the values of the ideality factor has increased after irradiation. Due to electron irradiation, the defects can be created in the crystal lattice and this causes an increase in the ideality factor. The increase in the barrier height is mainly responsible for the decrease in the reverse bias current of the diode. The radiation-induced degradation observed in the reverse I–V characteristics could be attributed to an increase in the interfacial defect density [8]. Furthermore, the increase in the barrier height and in the series resistance could be attributed to the deactivation of the dopant at the Au/n-Si interface. An increase in the ideality factor also indicates that for the diode, the current transport mechanism cannot be a thermionic emission type and it may be a tunnelling type transport [9].

The both forward bias I–V characteristics of the Schottky diode are linear but deviate considerably from the linearity due to some factors at large voltages, one of the factors is series resistance (R_s). One of the factors is series resistance is an important parameter on the electrical characteristics of the Schottky barrier contacts. The resistance of the Schottky barrier diode is the sum of total resistance value of the resistors in series and the resistance in the semiconductor device in the direction of current flow. The R_s is influenced by the presence of the interface layer between the metal and the semiconductor and leads to non-ideal forward bias C–V plots. When the applied voltage is sufficiently large, the effect of the R_s can be seen at the non-linear regions of the forward bias I–V characteristics. The Schottky diode parameters as the barrier height, the ideality factor, and the series resistance can also be achieved using a method developed by Cheung and Cheung [10].

According to [10], the forward bias I–V characteristics due to the TE of a Schottky diode with the series resistance can be expressed as

$$I = I_0\exp\left[\frac{q(V-IR_s)}{nkT}\right], \tag{5}$$

where the IR_s term is the voltage drop across series resistance of device. The values of the series resistance can be determined from the following functions using Eq. (5):

$$\frac{dV}{d(\ln I)} = \frac{nkT}{q} + IR_s, \tag{6}$$

$$H(I) = V - \left(\frac{nkT}{q}\right)\ln\left(\frac{I}{AA^*T^2}\right), \tag{7}$$

and $H(I)$ is given as follows:

$$H(I) = n\Phi_b + IR_s, \tag{8}$$

A plot of $\frac{dV}{d(\ln I)}$ vs. I will be linear and gives R_s as the slope and $\frac{nkT}{q}$ as the y-axis intercept from Eq. (6). Figs. 2 and 3 show the plots of $\frac{dV}{d(\ln I)}$ and $H(I)$ $vs.$ I for the unirradiated and irradiated cases. The values of n and R_s have been calculated as $n = 1.83$, $R_s = 214\ \Omega$ and $n = 1.98$, $R_s = 1149\ \Omega$, for before and after irradiation cases of the diode, respectively. It is observed that the value of n obtained from the forward-bias ln$I$–V plot is smaller than that of the dV/d(ln$I$)–I curves. This can be attributed to the effect of the series resistance and interface states, and to the voltage drop across the interfacial layer.

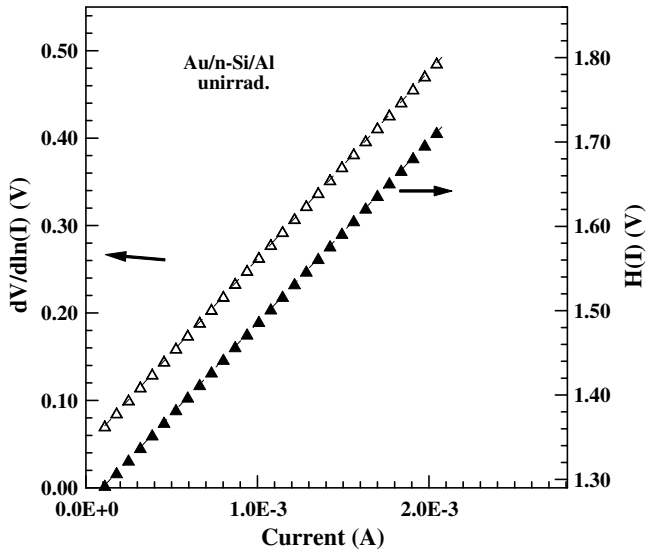

Fig. 2. A plot of $\frac{dV}{d(\ln I)}$ and *H(I) vs. I* obtained from the forward bias *I–V* characteristics of the Au/*n*-Si/Al diode before electron irradiation.

Besides, $H(I)$ vs. I plot has to be linear according to Ref. [8]. The slope of this plot gives a different determination of R_s. Using the value of the n obtained from Eq. (3), the value of Φ_b is obtained from the y-axis intercept. From $H(I)$ *vs. I* plots, the values of the Φ_b and R_s have been calculated as $\Phi_b = 0.76$ eV, $R_s = 216\ \Omega$ and $\Phi_b = 0.86$ eV, $R_s = 1153\ \Omega$, for the unirradiated and irradiated cases of the diode, respectively. It can be obviously seen that the values of R_s obtained from $H(I)$–I curve are in close agreement with the values obtained from the $dV/d(\ln I)$–I plot. But there is an increase in the series resistance value with the irradiation.

Norde [11] proposed an alternative method to determine the value of the series resistance. The following function has been defined in the modified Norde method:

$$F(V) = \frac{V}{\gamma} - \frac{kT}{q}\ln\left(\frac{I(V)}{AA^*T^2}\right), \tag{9}$$

where γ is an integer (dimensionless) greater than ideality factor. $I(V)$ is the current obtained from the I–V curve. Once the minimum of the F vs. V plot is determined, the value of barrier height can be obtained from Eq. (10), where $F(V_0)$ is the minimum point of $F(V)$ and V_0 is the corresponding voltage

$$\Phi_b = F(V_0) + \frac{V_0}{\gamma} - \frac{kT}{q}. \tag{10}$$

Fig. 4 shows the $F(V)$–V plot of the junction. From the Norde functions, R_S value can be determined as

$$R_S = \frac{kT(\gamma - n)}{qI}. \tag{11}$$

From the F–V plot, the values of Φ_b and R_s of the structure have been determined as 0.87 eV and 221 Ω for the unirradiated, and have been determined as 1.03 eV and 1341 Ω for the irradiated cases, respectively. There is an increase in the values of Φ_b and R_s after the electron irradiation. The value of series resistance indicates that the series resistance is a current-limiting factor for the Au/*n*-Si/Al Schottky diode. The effect of the series resistance is usually modelled with series combination of a diode and a resistance R_s. The nature of the I–V characteristics indicates that the resistivity of the material has increased after electron irradiation. This increase is attributed to the electron irradiation-induced defects, because the defects are created in the crystal lattice due to electron irradiation. Electron irradiation creates primarily displacement damage in the silicon lattice, which causes the generation of deep trap levels and hence a reduction in the carrier generation and recombination life time. The displaced atom leaves vacancy positions, which may migrate until they form stable configurations with impurity atoms [12]. Besides, this increase in the series resistance indicates that the product of the mobility and the free carrier concentration have reduced. The reduction in mobility is due to the introduction of defect centres on irradiation, which act as scattering centres [13]. At the same time, the decrease in the active dopant concentration, N_D, is responsible for the increase in the series resistance.

For the interface states in equilibrium with the semiconductor, the ideality factor n is given by [14]

$$n(V) = 1 + \frac{\delta}{\varepsilon_i}\left(\frac{\varepsilon_s}{w} + qN_{ss}(V)\right), \tag{12}$$

where ε_i and ε_s are the permittivities of interfacial layer and the semiconductor, w is the width of the space charge region and N_{ss} is the density of the interface states in equilibrium with the semiconductor. Furthermore, in n-type semiconductors, the energy of

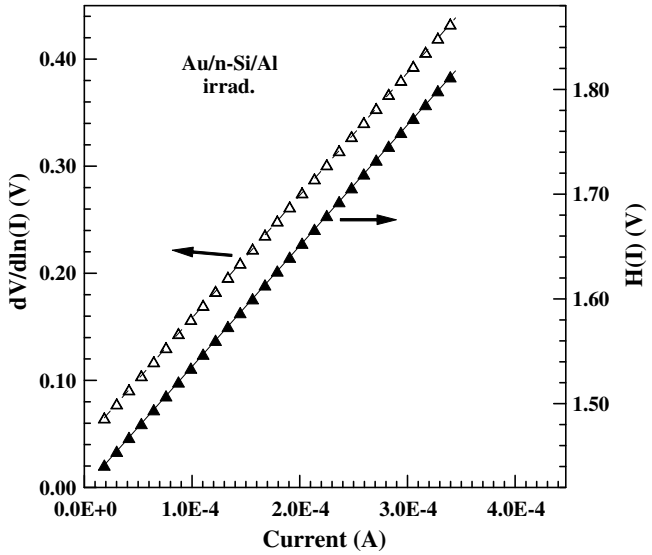

Fig. 3. A plot of $\frac{dV}{d(\ln I)}$ and *H(I) vs. I* obtained from the forward bias *I–V* characteristics of the Au/*n*-Si/Al diode after electron irradiation.

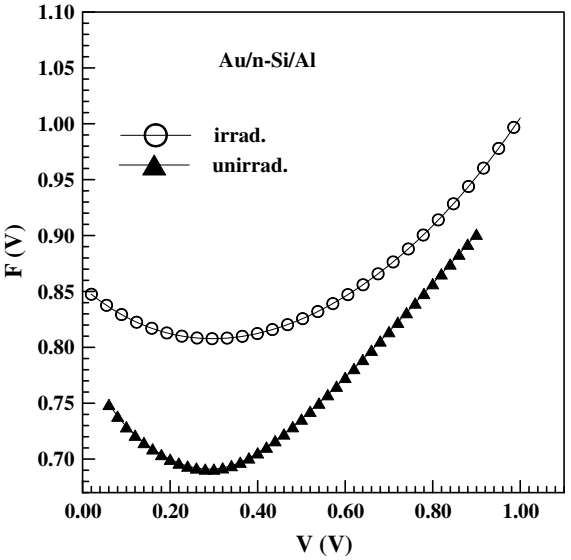

Fig. 4. *F(V)* vs. *V* plots of the Au/*n*-Si/Al Schottky diode for unirradiated and irradiated cases.

the interface states E_{ss} with respect to the bottom of the conduction band at the surface of the semiconductor is given by [15]

$$E_{SS} - E_v = q\Phi_e - qV. \tag{13}$$

The energy distribution or density distribution curves of the interface states can be determined from the experimental data of the forward bias the *I–V* characteristics. N_{ss} vs. E_{ss}–E_v plots of the Au/*n*-Si/Al Schottky diode are shown in Fig. 5. As can be seen in the figure, exponential growth of the interface sate density towards the top of the valance band is very apparent. The interface states, N_{ss}, have been decreased significantly after electron irradiation. It has been seen that the interface state densities have exponential rise with bias towards the top of the valence band. The interface state density N_{ss} obtained from the forward bias *I–V* ranges from 3.4×10^{14} to $7.7 \times 10^{14}\,cm^{-2}\,eV^{-1}$ for the unirradiated and 2.31×10^{14} to $5.91 \times 10^{14}\,cm^{-2}\,eV^{-1}$ for the irradiated situations, respectively. These changes have been attributed to the decrease in recombination centre and the existence of an interfacial layer between Au and *n*-Si semiconductor.

The analyses of the *C–V* characteristics have been achieved by using the following equation:

$$C^{-2} = \frac{2(V_d + V)}{\varepsilon_s \varepsilon_0 q A^2 N_d}, \tag{14}$$

where V_d is the diffusion potential at zero bias, which is determined from the extrapolation of the linear $1/C^2$-*V* plot to the *V*-axis; *A* is the effective area of the diode ($7.85 \times 10^{-3}\,cm^{-2}$); $_s$ is the dielectric constant of the semiconductor (= 11.7) for Si [16]; and N_d is the concentration of ionized donors. The value of the barrier height Φ_b can be calculated by the following well-known equation, using the *C–V* measurements:

$$\phi_b = V_d + V_n, \tag{15}$$

where V_n is equal to the Fermi energy level E_f, and can be calculated by knowing N_d and N_c, density of states in the conduction band, which is $N_c = 2.8 \times 10^{19}\,cm^{-3}$ for *n*-Si at room temperature [16].

Figs. 6 and 7 show the typical *C–V* characteristics for unirradiated and irradiated situations of the diode at various frequencies. It is seen from these figures that the values of the capacitance decrease with the increasing irradiation and frequency. This irradiation effect can be attributed to the change in dielectric constant at the metal semiconductor interface or to the decrease in the net ionized dopant concentration with irradiation [17–19]. Furthermore, the acceptor-like defects can be used to explain the decrease in the *C–V* properties of the Au/*n*-Si/Al diode after electron irradiation.

Fig. 8 depicts the reverse bias C^2–*V* characteristics of the unirradiated diode, at various frequencies. It is seen that the C^2–*V* are linear. This can be explained by the absence of the excess capacitance.

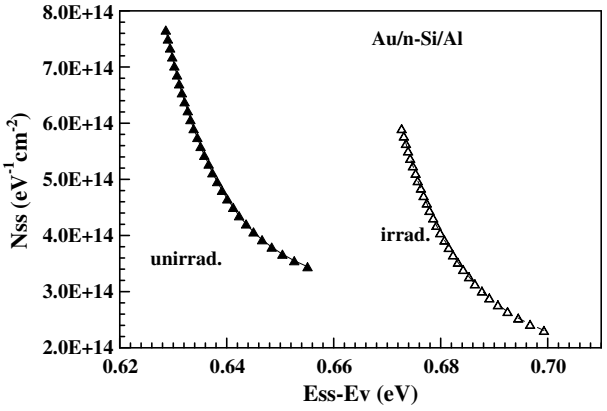

Fig. 5. *Nss* vs. *Ess–Ev* plots of the Au/*n*-Si/Al Schottky diode for unirradiated and irradiated cases.

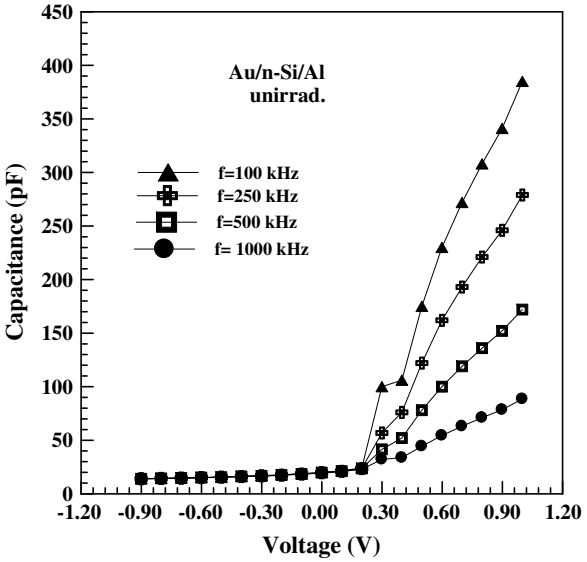

Fig. 6. The forward and reverse bias *C–V* characteristics of the Au/*n*-Si/Al Schottky diode before electron irradiation at various frequencies.

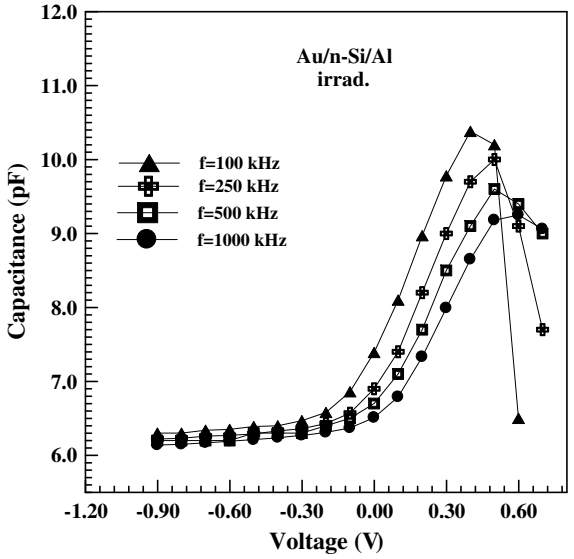

Fig. 7. The forward and reverse bias *C–V* characteristics of the Au/*n*-Si/Al Schottky diode after electron irradiation at various frequencies.

Fig. 9 shows the reverse bias C^2–*V* characteristics of the unirradiated and irradiated diode at only *f* = 1000 kHz frequency. After the irradiation, the intercept of the C^2–*V* characteristics shifts toward more positive voltages while the gradient remains almost constant. The lateral shift in the C^2–*V* characteristics is due to an increase in diffusion potential, which results in an increase in the barrier height. The donor (N_d) doping concentrations have been found as 6.62×10^{14}, and 2.27×10^{14} cm^{-3} for before and after electron irradiation, respectively at *f* = 1000 kHz frequency, using the following equation:

$$N_d = N_c \exp(V_n/kT). \tag{16}$$

The possible reasons for this reduction in carrier density may be the substitutional donors are moved into the interstitial site or the creation of the electron capture levels or acceptors-like defects at the interface of Au and *n*-Si.

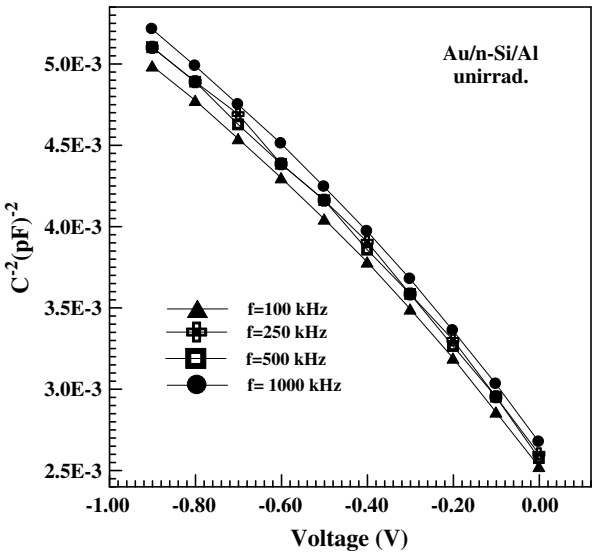

Fig. 8. The reverse bias C^{-2}–V characteristics of the Au/n-Si/Al diode before electron irradiation at various frequencies.

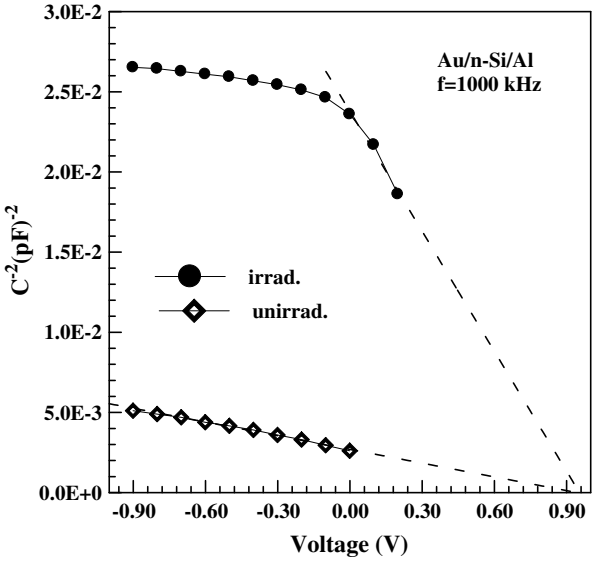

Fig. 9. The reverse bias C^{-2}–V characteristics of the before and after electron irradiation at f=1000 kHz frequency.

The values of the barrier heights obtained from the reverse bias C^{-2}–V characteristics at 1000 kHz frequency have been found as 0.82 and 1.08 eV for before and after irradiation, respectively. The values of the barrier heights extracted from the C–V curves are higher than that derived from the I–V measurements. This difference can be explained due to an interface layer or due to the barrier inhomogeneities [20]. According to Werner and Guttler, spatial inhomogeneities at the MS interface of abrupt Schottky contact can also cause such differences in the barrier height determined from I–V and C–V measurements [21].

Fig. 10 shows the C–f characteristics of the diode before and after electron irradiation, at various voltages. It is seen from these figures that the values of the capacitance have been decreased after electron irradiation. As described above, this state can be attributed to the change in dielectric constant at the interface or to the decrease in the net ionized dopant concentration with electron

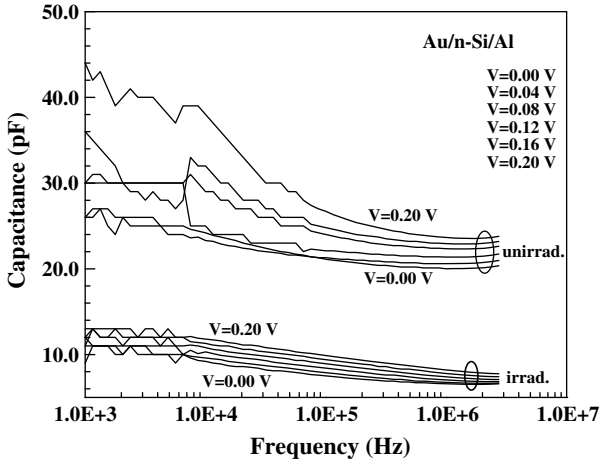

Fig. 10. The forward bias C–f characteristics of the Au/n-Si/Al diode before and after electron irradiation at various voltages.

irradiation. Besides, the higher values of capacitance at low frequency can be attributed to the interface states in equilibrium with the n-Si that can follow the alternating current signal, whereas at higher frequencies they cannot follow the alternating current signal. The values of the capacitance at the high frequency region originate from only the space charge capacitance.

4. Conclusion

It was found that the electrical characteristics of the Au/n-Si/Al Schottky diode are very sensitive to 6 MeV energy electrons irradiation. It was found that the values of Schottky barrier height, the series resistance, and the ideality factor showed an increase but the capacitance value showed a decrease after electron irradiation. The degradation in the Au/n-Si/Al diode properties may be due to the introduction of radiation-induced interfacial defects (between Au and n-Si), and lattice defects via displacement damage.

References

[1] A. Mogro-Campero, M.F. Chang, J.L. Benjamin, J. Electrochem. Soc. 135 (1988) 172–176.
[2] E. Ntsoenzok, J.F. Barbot, P. Desgardin, J. Vernois, C. Blanchard, D.B. Isabelle, IEEE Trans. Nucl. Sci. 41 (1994) 1932–1936.
[3] E. Ntsoenzok, P. Desgardin, M. Saillard, J. Vernois, J.F. Barbot, J. Appl. Phys. 79 (1996) 8274–8277.
[4] M. Yamaguchi, S.J. Taylor, M.J. Yang, S. Matsuda, O. Kawasaki, T. Hisamatsu, J. Appl. Phys. 80 (1996) 4916–4920.
[5] C. Claeys, E. Simoen, Radiation Effects in Advanced Semiconductor Materials and Devices, Springer Verlag, Berlin, Heidelberg, Germany, 2002.
[6] C. Coskun, N. Gedik, E. Balcı, Semicond. Sci. Technol. 21 (2006) 1656–1660.
[7] E.H. Rhoderick, R.H. Williams, Metal Semiconductor Contacts, second ed., Oxford, Clarendon, 1988.
[8] G.A. Umana-Membreno, J.M. Dell, G. Parish, B.D. Nener, L. Faraone, U.K. Mishra, IEEE Trans. Electron Dev. 50 (2003) 12.
[9] F. Roccaforte, S. Libertino, V. Raineri, A. Ruggiero, V. Massimino, L. Calcagno, J. Appl. Phys. 99 (2006) 013515.
[10] S.K. Cheung, N.W. Cheung, Appl. Phys. Lett. 49 (1986) 85.
[11] S. Karatas, S. Altindal, A. Turut, M. Cakar, Physica B 392 (2007) 43.
[12] M.J. Barrett, IEEE Trans. Nucl. Sci. NS-14 (1967) 82.
[13] M. Pattabi, S. Krishnan, Ganesh, X. Mathew, Sol. Energy 81 (2007) 111–116.
[14] J.C. Card, E.H. Rhoderick, J. Phys. D4 (1971) 1589.
[15] A. Singh, Solid-State Electron 28 (1985) 233.
[16] D.A. Neamen, Semiconductor Physics and Devices; Basic Principles, Irwin Inc., 1992. p. 144.
[17] O. Gullu, F. Demir, F.E. Cimilli, M. Biber, Vacuum 82 (2008) 789.
[18] S. Karatas, A. Turut, Nucl. Instrum. Meth. A 566 (2006) 584.
[19] P. Zukowski, J. Partyka, P. Wegierek, Phys. Stat. Sol. A 159 (1997) 509.
[20] C. Coskun, S. Aydogan, H. Efeoglu, Semicond. Sci. Technol. 19 (2004) 242.
[21] J.H. Werner, H.H. Guttler, J. Appl. Phys. 69 (1991) 1522.